Application of Depth-Averaged Bedload Finite-Volume Models to a Progressive Embankment Dam-Failure

Masoumeh Ebrahimi [(1)], Robin Meurice [(2)], and Sandra Soares-Frazão [(3)]

[(1)] Université Catholique de Louvain, Louvain-la-Neuve, Belgium
masoumeh.ebrahimi@uclouvain.be

[(2)] Université Catholique de Louvain, Louvain-la-Neuve, Belgium,
robin.meurice@uclouvain.be

[(3)] Université Catholique de Louvain, Louvain-la-Neuve, Belgium,
sandra.soares-frazao@uclouvain.be

Abstract

Overflowing and overtopping are the leading causes of failure of earthen dams and embankments. Especially in the context of climate change, these defense structures are more prone to extreme hydraulic loadings. Inundation hazard and risk map inherently depend on the dominant form of failure progression. Breaching of earthen dams or embankments is a complex phenomenon that relies on various characteristics such as constituted soil, hydraulic load, regular maintenance, etc.In the frame of the 6th workshop on River and Sedimentation Hydrodynamics and Morphodynamics, a blind benchmark test concerning progressive dam failure due to overtopping was offered to modelers in order to evaluate and calibrate their models. The present paper only reports about the simulations done at UCLouvain, during the blind phase of the benchmark test. Two depth-averaged finite-volume models were applied to this benchmark test. While the first model (WCM) decoupled the shallow-water equations from Exner's one, leaving only weak links between the different operators, the second one (CM) solved them altogether. The WCM was able to reproduce most of the reservoir's water level evolution and is hence supposed to rather accurately predict the evolution of the breach width. Conversely, the CM led to faster erosion of the dam than expected, which led to a rapid decrease of the reservoir's water level. Meanwhile, a bank-failure operator is necessary to reproduce properly the widening of the breach. Three sediment transport formulas are used to observe their influence on the erosion rate of the embankment.

Keywords: breaching, dam-failure, embankment dam, finite-volumes, overtopping.

1. INTRODUCTION

Embankment dams are very common worldwide to form reservoirs or along rivers to protect the adjacent lands from inundation or guarantee inland navigations. Yet, the stability of these dams can be jeopardized through different failure mechanisms (ASCE/EWRI, 2011). Moreover, the point of no return can be reached very rapidly and lead to progressive or sudden failure of the dam depending on the failure mechanism. Not only will the downstream reach then be subject to catastrophic flooding but the collapsed soil could worsen the downstream impacts. Risk management and emergency response require the knowledge of the outflow hydrograph as accurate as possible. Therefore, physically-based models considering all aspects are essential to calculate appropriately the breaching hydrograph (Wahl, 1998).

The complexity of failure of earthen dams and embankments also necessitate experimental studies either at a laboratory or real scale. One recent experimental study (Alvarez et al. 2022) was performed in the laboratory facility of Laboratório Nacional de Engenharia Civil (LNEC) , located in Lisbon, Portugal. This test consisted of the failure by overtopping of an earthen dam with a breach in the middle of its crest and through which the erosion of the dam would progressively develop, vertically and laterally, as the discharge at the inlet of the reservoir was increasing. This benchmark test provides modelers with essential data to evaluate and calibrate their model. Besides, attempts at improving current knowledge and understanding the models' limitations may facilitate the road toward developing more sophisticated models.The models are supposed to reproduce properly the deepening and widening of the breach.

During the first blind stage, only limited data, such as dam dimensions, boundary conditions and water level in the reservoir, were provided to the modelers and hence, raw results were expected. Thus, this paper is not concentrated on validating the two models through detailed comparisons with measured data but instead

investigating the sensitivity of the results to different modeling options. Arousing questions regarding the influence of soil cohesion and erodibility, sediment size and distribution, the sensitivity of crest height to water level banks' instabilities, and mesh size were tried to address.
To this end, a numerical model consisiting of Saint-Venant's equations and Exner's equation (already developed by UCLouvain hydraulic research team) was applied to simulate breaching process. The process basically is entrainmaint of sediments into the flow and being transported predominantly in bedload form (Broich 1998; Tingsanchali & Chinnarasri, 2001; Soares-Frazão & Zech, 2011). The model was originally developed for granular sandy soil with a uniform grain-size distribution with a Clear Water Layer model (CWL) assumption which implies that a layer of water free of sediment flows over the mobile sediment bed. Therefore, sediment transport in suspension is not implemented in solid discharge.
The equations are solved using an explicit 2D finite-volume method on unstructured triangular grids, with HLLC flux calculation in two slightly different manner called as Coupled Model and Weakly Coupled Model. While the first model (CM) solved them altogether, the second one (WCM) decoupled the shallow-water equations from Exner's one, leaving only weak links between the different operators.

2. GOVRNING EQUATIONS

The two-dimensional shallow water equations describe mass and momentum conservation for water in partial differential form for an arbitrary cross-section (see Eq. [1-3]):

$$\frac{\partial h}{\partial t}+\frac{\partial q_x}{\partial x}+\frac{\partial q_y}{\partial y}=0 \qquad [1]$$

$$\frac{\partial q_x}{\partial t}+\frac{\partial \sigma_x}{\partial x}+\frac{\partial \mu_{xy}}{\partial y}= gh(S_{0,x}-S_{f,x}) \qquad [2,a]$$

$$\frac{\partial q_y}{\partial t}+\frac{\partial \sigma_y}{\partial y}+\frac{\partial \mu_{xy}}{\partial x}= gh(S_{0,y}-S_{f,y}) \qquad [2,b]$$

The sediment continuity is guaranteed through the Exner equation:

$$\frac{\partial z_b}{\partial t}+\frac{1}{(1-\varepsilon_0)}\frac{\partial q_{s,x}}{\partial x}+\frac{1}{(1-\varepsilon_0)}\frac{\partial q_{s,y}}{\partial y}=0 \qquad [3]$$

with *h* being the water depth, q_x and q_y the unit discharge components in the *x* and *y* directions respectively, *g* the gravitational acceleration, σ_x and σ_y the normal momentum fluxes in the *x* and *y* directions respectively, μ_{xy} the transverse momentum flux, $S_{0,x}$ and $S_{0,y}$ the bed slope in the *x* and *y* directions respectively, and *u* and *v* the depth-averaged velocity components in the *x* and *y* directions respectively. The bottom friction closure equation integrated into the model in two directions is expressed by $S_{f,x}=\frac{n^2\sqrt{u^2+v^2}u}{h^{4/3}}$ and $S_{f,y}=\frac{n^2\sqrt{u^2+v^2}v}{h^{4/3}}$, explicitly calculated with the Manning coefficient *n*, z_b the bed level, $q_{s,x}$ and $q_{s,y}$ the unit solid discharge components and ε_0 the bed porosity.
Another closure equation to be considered is the sediment transport rate. Several sediment transport formulas are implemented to better predict the failure progression and water level evolution in the reservoir. These formulas include Meyer-Peter and Müller (MPM) (1948), Van Rijn (1984) Wong and Parker (2006). Moreover, the critical shear stress was adapted according to the upper boundary found by Ansari et al. (2007) for a relatively similar grain size distribution:
The sediment transport formulas used (only in the *x*-direction) in the coupled model are:

$$q_{s,x}=8\sqrt{g(s-1)d_{50}^3}\left(\frac{n^2q_x(q_x^2+q_y^2)^{1/2}}{(s-1)d_{50}h^{7/3}}-\tau_{*c}\right)^{3/2} \qquad [4]$$

$$q_{s,x}=0.00033(\sqrt{g(s-1)d_{50}^3})d_{50}{}^{0.3}\left[\frac{(s-1)g}{\vartheta^2}\right]^{1/10}\left(\frac{n^2q_x(q_x^2+q_y^2)^{1/2}}{(s-1)d_{50}h^{7/3}\tau_{*c}}-1\right)^{3/2} \qquad [5]$$

where $\tau_{*c}=0.047$ with MPM (Eq. [5]) and $\tau_{*c}=0.26$ with Van Rijn (Eq. [6]).

The Wong and Parker (2006) formula is as follows:

$$q_{s,x}=3.97\sqrt{g(s-1)d_{50}^3}\left(\frac{n^2q_x|q_x|}{(s-1)d_{50}h^{7/3}}-\tau_{*c}\right)^{3/2} \qquad [6]$$

with $\tau_{*c} = 0.26$ according to Ansari et al. (2007).

3. NUMERICAL RESOLUTION

3.1 Coupled model

The Saint-Venant-Exner (SVE) equations are solved simultaneously so it is called a coupled model. The governing equations [1] to [3] are written in vector form (Eq.(7)):

$$\frac{\partial \boldsymbol{U}}{\partial t} + \frac{\partial \boldsymbol{F}(\boldsymbol{U})}{\partial x} + \frac{\partial \boldsymbol{G}(\boldsymbol{U})}{\partial y} = \boldsymbol{S} \qquad [7]$$

where,

$$\boldsymbol{U} = \begin{pmatrix} h \\ q_x \\ q_y \\ z_b \end{pmatrix}, \boldsymbol{F} = \begin{pmatrix} q_x \\ \sigma_x \\ \mu_{xy} \\ q_{s,y}/(1-\varepsilon_0) \end{pmatrix} \qquad [8a,b]$$

$$\boldsymbol{G} = \begin{pmatrix} q_y \\ \mu_{xy} \\ \sigma_y \\ q_{s,y}/(1-\varepsilon_0) \end{pmatrix}, \boldsymbol{S} = \begin{pmatrix} 0 \\ gh(S_{0,x} - S_{f,x}) \\ gh(S_{0,y} - S_{f,y}) \\ 0 \end{pmatrix} \qquad [8c,d]$$

These equations are then discretized according to a first-order finite-volume scheme (Eq.[9]) that is run on a two-dimensional mesh composed of unstructured triangular cells (Figure 1), as generated e.g. by the software Gmsh (Geuzaine and Remacle 2009).

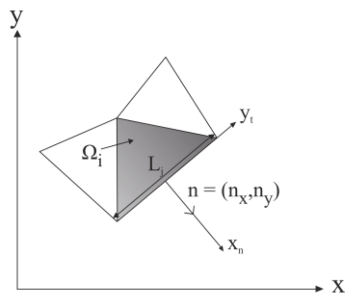

Figure 1: coordinate system local to the intercell edge.

$$\boldsymbol{U}_i^{n+1} = \boldsymbol{U}_i^n - \frac{\Delta t}{\Omega_i} \sum_{j=1}^{nb} \boldsymbol{T}_j^{-1} \boldsymbol{F}_j^{*}(\overline{\boldsymbol{U}}_j) L_j + \boldsymbol{S}_{F,i} \Delta t \qquad [9]$$

Where $\boldsymbol{\Omega_i}$ the cell-based area, *j* the considered cell interface, $\boldsymbol{L_j}$ the $\boldsymbol{j}$-interface length, $\boldsymbol{nb}$ the number of cell interfaces. The stability is dictated by the CFL condition (Courant et al., 1967). To calculate the mass and momentum fluxes at the interfaces, a lateralized HLLC solver (Harten et al.,1983) is included in the model.

3.2 Weakly Coupled model

The Exner equation can also be solved as a next step to the resolution of the shallow water equations. Juez et al. (2014) decoupled the hydrodynamic and sedimentological equations in such a way that only the hydrodynamic quantities involved in mass and momentum conservation laws were coupled in equation [8], whereas the Exner equation [3] is handled separately.

The method is adapted to the lateralized HLLC solver (Meurice & Soares-Frazão, 2020) instead of the Roe-type solver used by Juez et al. (2014). The bed evolution is calculated with a first-order finite-volume method as follows:

$$z_{b,i}^{n+1} = z_{b,i}^{n} - \frac{\Delta t}{\Omega_i}\sum_{j=1}^{nb}\frac{1}{1-\epsilon_0}q_{s,n,j}^{*}L_j \quad [10]$$

Where

$$q_{s,n,j}^{*} = \begin{cases} q_{s,n,L} \; if \; \tilde{\lambda}_{s,n,j} \geq 0 \\ q_{s,n,R} \; if \; \tilde{\lambda}_{s,n,j} < 0 \end{cases} \quad [11]$$

with $q_{s,n,L}$ and $q_{s,nR}$ being the components of the unit normal solid discharges to the left and right sides of cells respectively.

3.3 Bank-failure operator (BFO)

A bank-failure operator developed by Swartenbroeckx et al. (2010) which accounts for the failure of the local steep slopes based on simple geotechnical considerations, is integerated into the model. The operator, indeed, verifies that the local cell inclination is kept in limits of stability angles after each erosion or deposition update. The unstable bed elements are tilted around an appropriate axis, ensuring mass conservation. The key parameters of this operator are the emerged and submerged angles of repose of the bed material, that can be adjusted to control the rate at which bank collapse occur in the model. Adding advantage of this operator to the model is the rotation of unstable elements of the banks, allowing failure progression laterally and therefore avoiding unphysical vertical walls. This is more clearly illustrated in the results.

4. EXPERIMENTAL SETUP

A homogenous dam-breach benchmark test under overtopping has conducted recently by Alvarez et al. 2022, at the LNEC laboratory in Portugal during the 6th Workshop on River and Sedimentation, Hydrodynamics and Morphodynamics (Figure 2). Information provided to the modellers comprised the dam layout, boundary conditions, and soil properties found in Table 1. The dam height is 45 cm with a base length of 2.20 m. The crest width is 0.17 m and the upstream and downstream slopes are respectively 1:2 and 1:2.5 (V:H). An initial notch with 1:1 side slope (indicated as *zoom* in the figure) was made through the entire length of the crest to guide the flow and initialize the process appropriately.

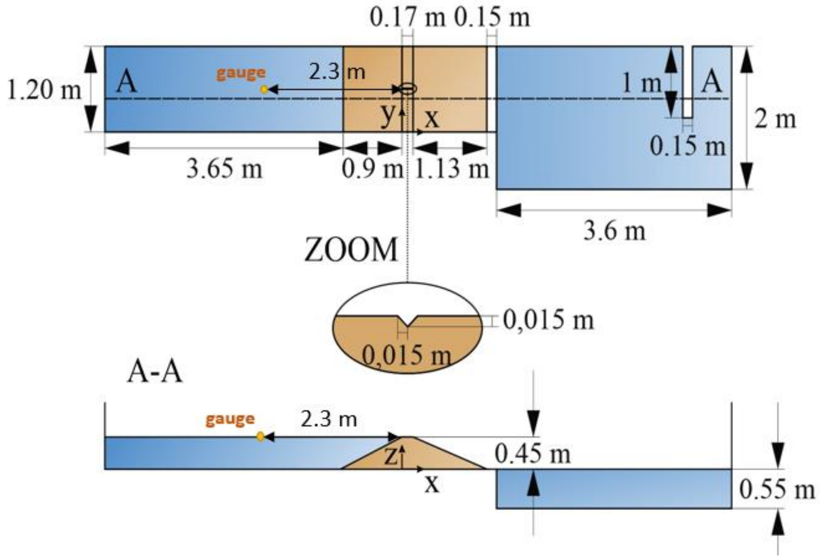

Figure 2: Experimental setup for the homogenous dam.

Table 1: Soil characteristics

Soil Type	Silty Sand (25% fine)	**Critical shear stress**	36.7 N/m^2
d_{50}	0.32 mm	**Friction angle**	30-35°
Relative compaction (Proctor compaction test)	90%	**Liquid limit**	17 (non-plastic) Non-cohesive soil

The results concerning the application of the CM and WCM models to the first test are mentioned hereunder. The mesh was generated in Gmsh (Figure 3) and appropriate boundary conditions were applied to the inlet, outlet and walls. A continuous and increasing discharge (shown in Figure 4) was provided at the inlet (a) with an initial water level equal to 45 cm. At the outlet (b), the water was free to flow.Figure 5 also shows the measured water elevation in the upstream reservoir, that was provided to the modellers. It can be observed that this leval remains almost constant for about 2500 s, and then the failure really starts, leading to a rapid increase of the inflow discharge to maintain the reservoir level as constant as possible.

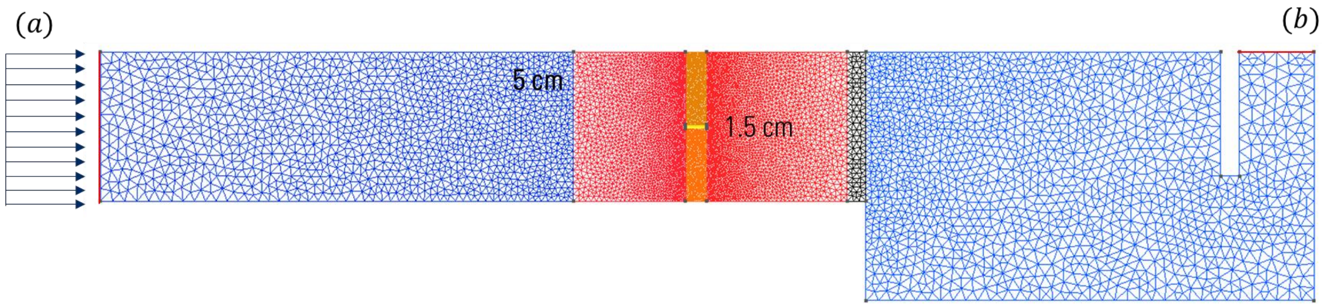

Figure 3: Unstructured triangular mesh.

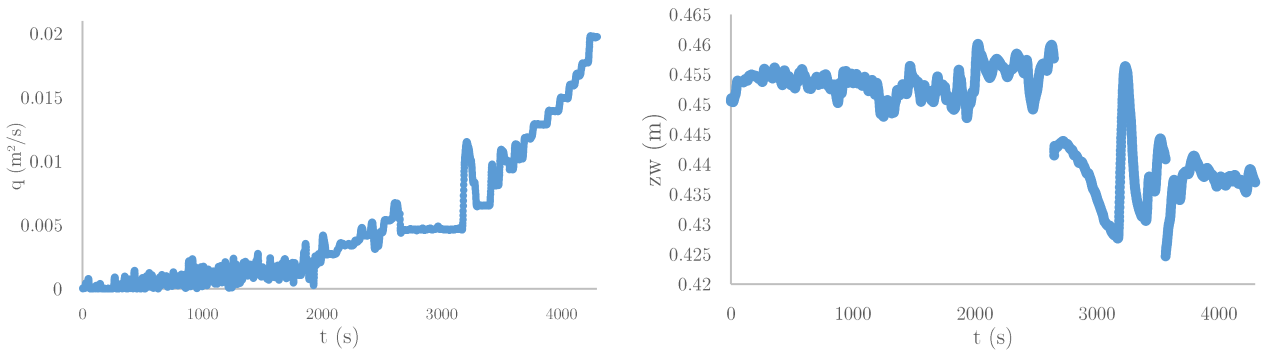

Figure 4: Water discharge (q) at the inlet (first graph), and water level measurement (zw) as a function of time in the reservoir at the gauge.

5. Results and discussions

A series of steps are taken to improve the results obtained by the numerical model not only in terms of physical parameters linked to the dam dimensions and soil characteristics but also in terms of the model itself. Among these, a minimum number of sediment transport formulas are employed to enhance the erosion rate in parallel to the augmentation of the critical shear stress. On the other hand, some limitations of the CM is surpassed through applying the coupled model. However, figuring out further improvements is the goal of the calibration phase of the models.

5.1 CM results

The coupled model is used to run the first series of simulation considering non-cohesive soil and a fixed diameter representing the grain distribution. The influence of the bank-failure-operator is also studied to see any improvement.
The simulations started with the original parameters of the dam, i.e., considering a crest level of 45 cm, using the classical MPM sediment transport formula, and in the absence and presence of bank-failure operator. The illustrations of Figure *5* show that the flow passes over the entire width of the dam leading to the uniform erosion of the dam. There are some instabilities in both cases around the crest moving downstream of the dam after activating the BFO. Another interesting observation is that the BFO could also worsen the condition when the whole width of the dam is overtopped and resulting to even higher dam erosion. Correspondingly, the dam is eroded up to 50 % of its height during the first 200 seconds (right figure). Therefore, the initial notch, alone, was not enough to lead the flow and start the breaching in this situation.

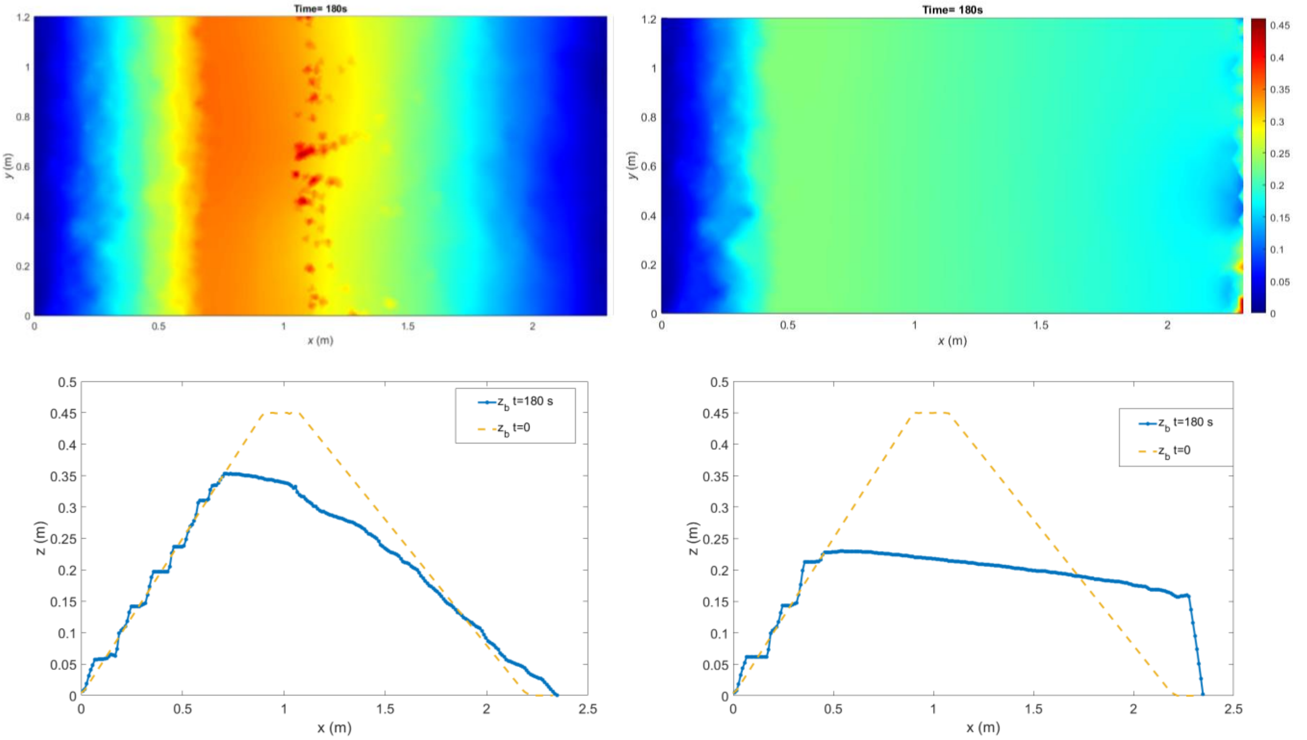

Figure 5: Plan view(xy) and longitudinal profile(xz) of the dam-breach simulation using the CM at time 180 s without (left side) and with (right side) bank-failure operator (MPM formula and a 45-cm-crest height)

Due to the rapid erosion of the dam and the effectiveness of BFO at this stage, some parameters were modified in the following order: (i) crest level was raised to 46 cm (ii) adjusting the repose angles of the bank-failure operator. Results are improved significantly by changing the crest level to 46 cm. As shown in Figure 6a, the breach forms completely and the surface erosion occurs at the downstream. However, the bank-failure operator is essential to see the lateral widening of the breach, especially through the crest, as illustrated in Figure 6b,c.

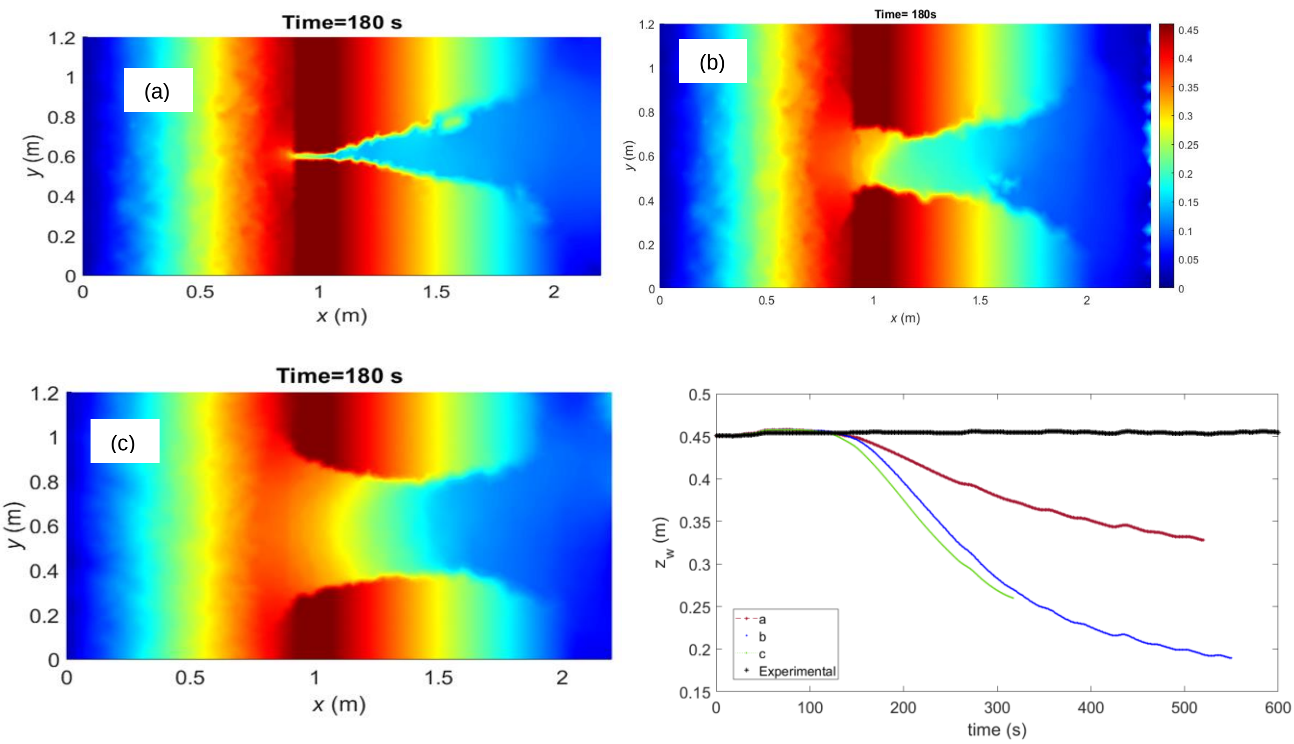

Figure 6 Plan view of the 46-cm-crest-height dam-breach simulation using the CM model using MPM formula: a) without BFO; b) with BFO and increased repose angles;c) with BFO and classical repose angles.

The repose angles are as follows: respectively corresponding to Figure 6 b and c $\alpha_{ce} = 87°$, $\alpha_{re} = 85°$, $\alpha_{cs} = 60°$, $\alpha_{rs} = 60°$ and $\alpha_{cs} = \alpha_{rs} = 30°$ (same as the internal friction angle) $\alpha_{ce} = 87°$, $\alpha_{re} = 85°$. Steeper $\alpha_{cs} = \alpha_{rs}$ angles decrease, on the one hand, the widening rate of lateral erosion of the breach, and on the other hand, the walls are more vertical, as is the case in the experiments. Yet, the results are not convincing since the dam eroded entirely before the experiment duration, and the lateral enlargement is significant. Besides, the water level falls highly during the first 500 seconds.
Thus, the dam has remained at 46 cm height since it results in better outcomes, but further modifications are applied in addition to those previously explained. One of the criteria that influence the results is the choice of the sediment transport formula itself. Moreover, all of these formulas contain a threshold parameter, critical shear stress, from which the flow will carry the sediments. So in the following paragraph, the results concerning the application of the formula obtained by Van Rijn (1984) and the modified non-dimensional shear stress are mentioned.
Van Rijn formula has been tested to compare the influence of the sediment entrainment process and as an effort to improve the results in terms of erosion rate and water level evolution in the reservoir. The Van Rijn (1984) formula rewritten in Eq. [6] with a modified non-dimensional critical shear stress, as well as higher stability angles ($\alpha_{ce} = 87°$, $\alpha_{re} = 85°$, $\alpha_{cs} = 80°$, $\alpha_{rs} = 45°$) were applied to the code. The erosion rate decreases significantly and the dam remains in place for the entire experiment duration. Some unphysical heaps form just before the downstream reservoir which does not impact the procedure due to the important stability angles (see Figure 7).

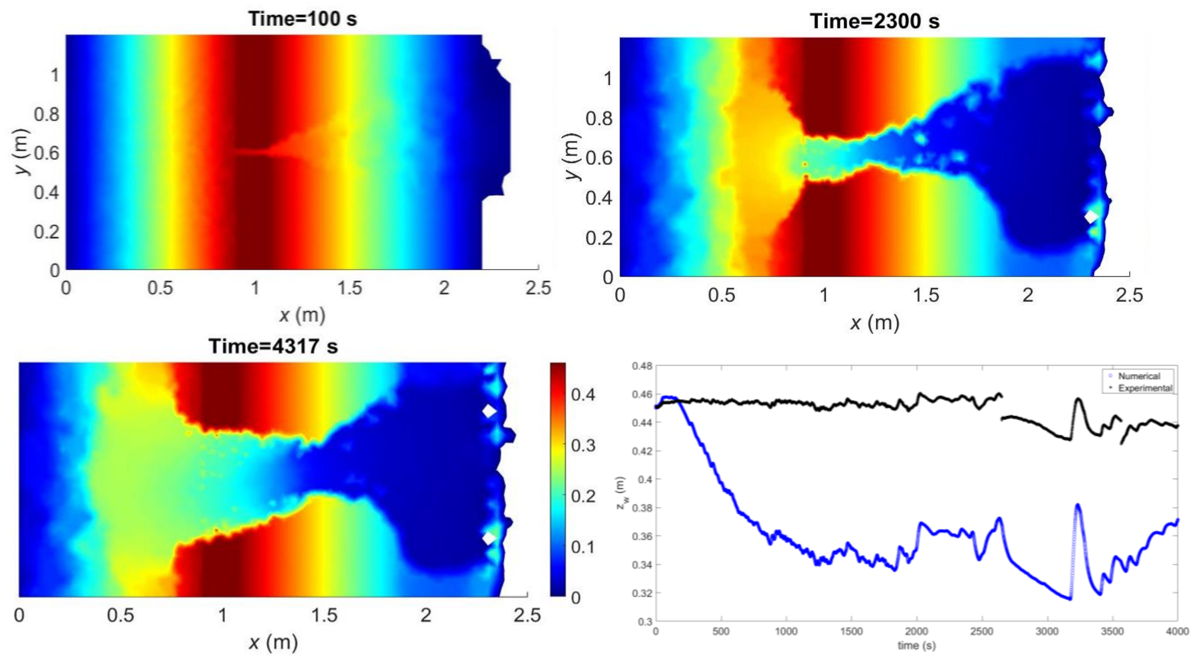

Figure 7: Dam evolution in 2D using Van Rijn's formula at three different times; comparative water level evolution in reservoir (last graph).

In terms of water level in the reservoir (Figure *7*), it falls up to 10 cm at the beginning which is related to the rather high erosion rate . Despite a fall of 10 cm until 1000 s the trend is well reproduced and water level is oscilating around a constant value. Nevertheless, the erosion rate is still high compared to the experimental tests which guided the simulations toward utilasation of the weekly coupled model.

5.2 WCM results

The WCM model runs to reproduce and enable the observed water level evolution in the reservoir. It was appeared almost impossible when using the prescribed soil parameters: the resulting failure was much faster than the observed one, the latter being probably slower due to some apparent cohesion of the dike material, that the model could not reproduce. Therefore, the parameters of the bank failure were adjusted based on the previous observations (Table 2). Once again, the model was run with and without the bank failure operator. The results are illustrated in Figure 8 (without bank failure operator) and Figure 9 (with bank failure operator, using the parameters defined in Table 2). Apart from these modifications, the solid discharge closure formulation was that of Wong and Parker (2006) in all simulations made with the WCM.

The results produced without the bank-failure operator finally gave the closest water level time series with the experimental data. Nevertheless, the morphology downstream of the breach showed unphysically straight heaps of soil. Those with the bank-failure operator showed fewer unphysical irregularities, but the difference between the experimental and numerical water level time series was higher.

Table 2: Repose angles for the bank-failure operator in the WCM

α_{ce}	$87°$
α_{cs}	$80°$
α_{re}	$85°$
α_{rs}	$45°$

For each data set, the evolution of the bed level is illustrated by three pictures.

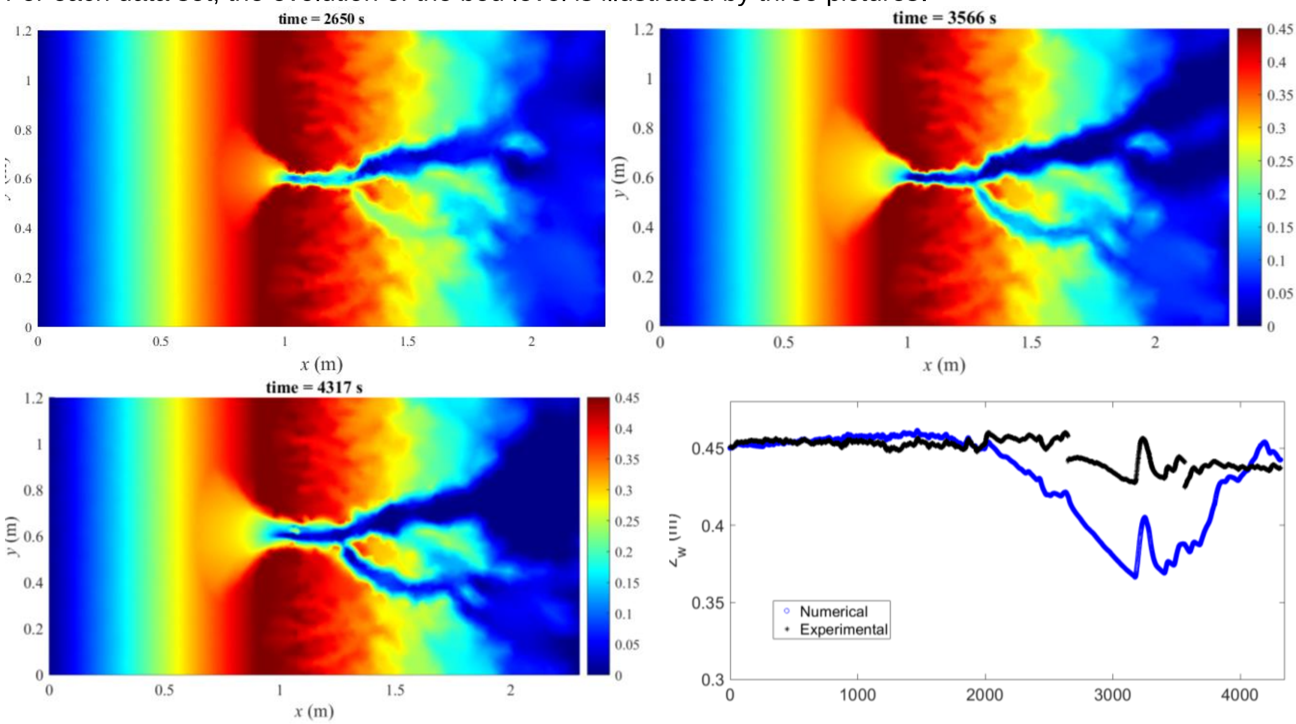

Figure 8: Plain view of the bed elevation (m) as computed by the model without the bank-failure operator at three different times,and water level evolution comparision(last figure) in the reservoir.

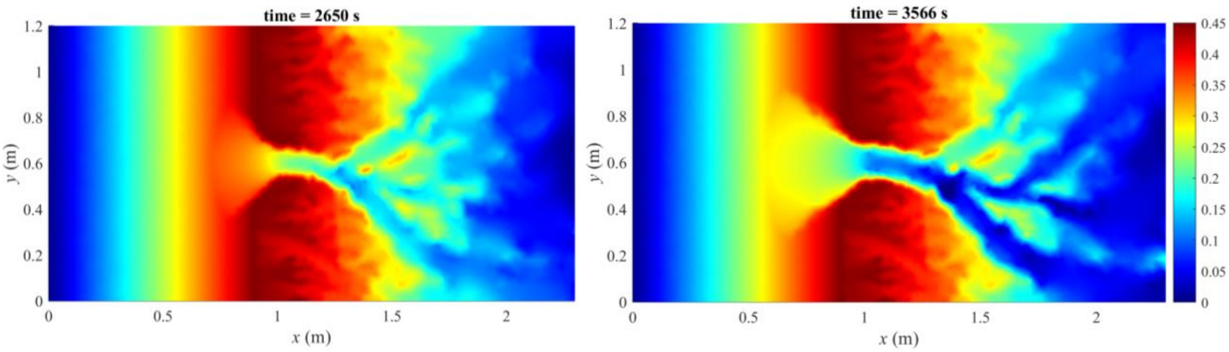

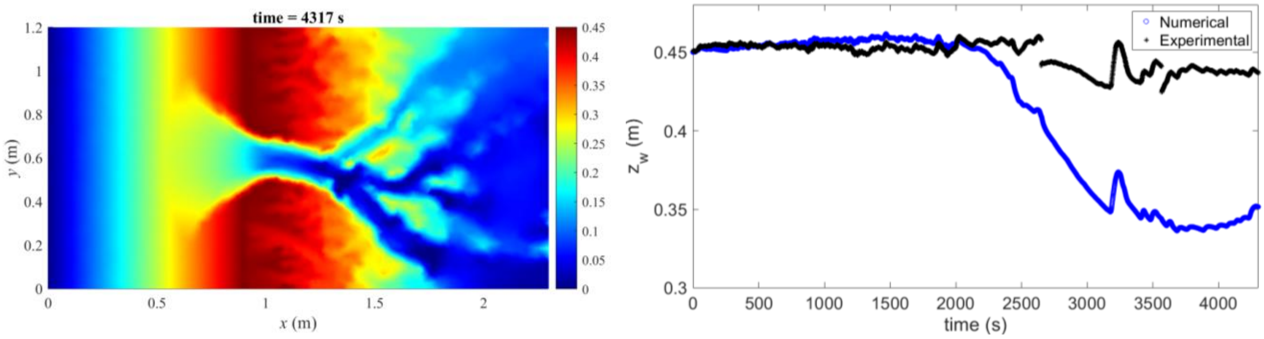

Figure 9: Plan view of the bed elevation (m) as computed by the model with the bank-failure operator at three different times, and comparative water level evolution (last graph) in the reservoir.

Both variations of the model show some asymmetry in the results, and the formation of diverging channels following the erosion of the downstream face of the dike. Without the bank failure operator, the banks become steep as only bed erosion is allowed in the model, and the water level remains the best. In the case with bank failure operator, the parameters were adjusted as indicated in Table 2, with very steep angles, hence producing results that appear quite close to the ones without the bank failure operator. This optoion allowed to delay the failure of the dike, but resulted in probably unphysical erosion patterns.

The two CM and WCM models have some limitations when applied to the benchmark dam. All these limitations can be justified by looking at the characteristics of the soil and other physical aspects such as apparent cohesion, dam compaction, and grain distribution. The detailed explanation and experiments visualization made during the online workshop is valuable and helpful to improve the models as far as possible because not all of them are already formulized to the authors' knowledge.

6. CONCLUSIONS

Two finite-volume models solving the shallow water and Exner equations in a coupled and weakly-coupled way were applied to a dam-breach benchmark test, that was conducted in a blind way. A series of modifications were made to the model parameters to approach experimental water level evolution in reservoir. Some of these modifications are the choice of sediment transport formulas, critical shear stress, lateral erosion parameters related to bank-failure operator, dam height (only in CM).

The WCM could reproduce the reservoir's water level evolution well and could better predict the breach discharge and potentially width growth while the CM produces a more realistic breach widening, however too fast. Therefore, the CM led to faster dam erosion than expected, leading to a rapid decrease in the reservoir's water level. Nevertheless, the CM showed fewer oscillations on the downstream slope of the dam once it was eroded. The WCM produced braided channels on the downstream face of the dike, with unphysical remnants of the dike's initial slope.

A bank-failure operator was used with both models. This operator failed to wash these unphysical soil heaps out for the WCM, but induced and increase of the breach's width, which negatively impacted the correspondence between the experimental and numerical reservoir's water level. Proper calibration of this bank-failure operator to cope with the apparent cohesion and avoid unphysical soil heaps should be performed during the calibration stage to follow the current blind step of the benchmark. The dam compaction also significantly influences the erodibility of the sediments but is not accounted for in usual sediment transport formulas.

A calibration phase will follow this first blind test, that will include investigation of mesh size refinement, and the use of different sediment transport formulation that could possibily account for cohesion and compaction. This second step should deliver more in-depth comparisons between the models' results and the experimental data considering the blind phase as a bonus to better understand all shortages of current models.

7. ACKNOWLEDGEMENTS

The authors would like to acknowledge the IST and LNEC team for proposing this benchmark test.

8. REFERENCES

Alvarez, T.; Mendes, S.; Aleixo, R.; Amaral, S.; Caldeira, L.; Viseu, T.; Ferreira, R.M.L. (2022) Hydraulics and Morphodynamics of Overtopped Dams with Chimney Filter. Proc. Proceedings of the 39th IAHR World Congress 19-24 June 2022 Granada, Spain, paper ID1466.

Ansari, S. A., Kothyari, U. C., & Ranga Raju, K. G. (2007). Incipient motion characteristics of cohesive sediments. ISH Journal of Hydraulic Engineering, 13(2), 108-121.

ASCE/EWRI Task Committee on Dam/Levee Breaching (2011). Earthen Embankment Breaching. J. Hydraul. Eng., ASCE, forum paper, 137(12), 1549–1564.

Broich, K. (1998). “Mathematical modeling of dam-break erosion caused by overtopping.” M. Morris, ed., CADAM-Concerted Action on Dambreak Modeling: 2nd Project Workshop, Munich, Germany.

Costanzo C., Macchione F. & Viggiani G. 2002 The influence of source terms treatment in computing two-dimensional flood propagation. Proceedings of the International Conference on Fluvial Hydraulics River Flow, 277-282.

Courant, R., Friedrichs, K., & Lewy, H. (1967). On the partial difference equations of mathematical physics. IBM journal of Research and Development, 11(2), 215-234.

Fraccarollo L., Capart H. & Zech Y. 2003 A Godunov method for the computation of erosional shallow water transients. International Journal for Numerical Methods in Fluids. 41(9), 951-976. DOI: 10.1002/fld.475.

KY.Geuzaine C. & Remacle J.-F. 2009 Gmsh: a three-dimensional finite element mesh generator with built-in pre- and post-processing facilities. International Journal for Numerical Methods in Engineering. 79(11), 1309-1331. DOI: 10.1002/nme.2579.

Juez, C., Murillo, J., & García-Navarro, P. (2014). A 2D weakly-coupled and efficient numerical model for transient shallow flow and movable bed. Advances in Water Resources, 71, 93-109.

Meurice, R., & Soares-Frazão, S. (2020). A 2D HLL-based weakly coupled model for transient flows on mobile beds. Journal of Hydroinformatics, 22(5), 1351-1369.

Meyer-Peter E. & Müller R. 1948 Formulas for Bed-Load Transport. Proc., 2nd Meeting IAHF, Stockholm.

Rijn, Van and C. Leo. “Sediment transport; Part I, Bed load transport.” Journal of Hydraulic Engineering 110 (1984): 1431-1456.

Soares-Frazão S., Zech Y. (2011) “HLLC scheme with novel wave-speed estimators appropriate for two-dimensional shallow-water flow on erodible bed”, International Journal for Numerical Methods in Fluids, 66(8), 1019–1036.

Swartenbroekx, C., Soares-Frazão, S., Staquet, R., & Zech, Y. (2010). Two-dimensional operator for bank failures induced by water-level rise in dam-break flows. Journal of Hydraulic Research, 48(3), 302-314.

Tingsanchali, T., and Chinnarasri, C. (2001). “Numerical modeling of dam failure due to flow overtopping.” Hydrol. Sci. J., 46(1), 113–130.

Wahl, T. L. (1998). “Prediction of embankment dam breach parameters: A literature review and needs assessment.” Dam Safety Rep. No. DSO-98-004, Bureau of Reclamation, U.S. Dept. of the Interior, Denver.

Wong, M., & Parker, G. (2006). Reanalysis and correction of bed-load relation of Meyer-Peter and Müller using their own database. Journal of Hydraulic Engineering, 132(11), 1159-1168.